

Electronic States in a Doubly Eccentric Cylindrical Quantum Wire

R. Kumar^{1*}, S. N. Singh²

¹Department of Physics, St. Xavier's College, Ranchi-834001, India

²Department of Physics, Ranchi University, Ranchi-834001, India

Received 15 February 2020, accepted in final revised form 5 June 2020

Abstract

Electronic states of a single electron in doubly eccentric cylindrical quantum wire are theoretically investigated in this paper. The motion of electron in quantum wire is free along axial direction in a cylindrical quantum wire and restricted in annular regions by three different parallel finite cylindrical barriers as soft wall confinement. The effective mass Schrödinger equation with effective mass boundary conditions is used to find energy eigenvalues and corresponding wavefunctions. Addition theorem for cylindrical Bessel functions is used to shift the origin for applying boundary conditions at different circular boundaries. Fourier expansion is applied after addition theorem to get wavefunctions in analytical form. A determinant equation is obtained as a result of applications of effective mass boundary conditions which roots gives energy of various electronic states. The lowest root gives ground state energy. The variation in ground state energy with eccentricity is obtained numerically and presented graphically. Electronic states in massive wall confinement and hard wall confinement is further obtained as limiting behavior of the states obtained in soft wall confinement. The knowledge of electronic states in such cylindrical hetrostructures semiconductor material can lead to improve the efficiency of many quantum devices.

Keywords: Doubly eccentric quantum wire; Addition theorem; Effective mass Schrödinger equation; Soft wall confinement; Bessel functions.

© 2020 JSR Publications. ISSN: 2070-0237 (Print); 2070-0245 (Online). All rights reserved.

doi: <http://dx.doi.org/10.3329/jsr.v12i4.45504>

J. Sci. Res. **12** (4), 473-483 (2020)

1. Introduction

The semiconductor hetrostructures are very useful in construction of many quantum devices like quantum laser where active medium is a quantum wire or dot. A lot of properties of quantum wire has been studied. Optical properties of a cylindrical quantum wire has been investigated theoretically to study variation of absorption coefficient and refractive index [1,2]. Binding energies of impurity in quantum dot structures have been studied as function of geometry [3]. Effect of shape and size on electron energy spectrum

*Corresponding author: rkumariitm@gmail.com

in various shaped quantum structures have been investigated [4-8]. The properties of quantum wire and dots with cylindrical geometry are of special interests among various researchers due to its wide range of applications [9-15]. Theoretical study of electrical properties of single eccentric cylindrical structures with C_{1v} and $C_{\infty v}$ symmetries have been studied [16]. We have investigated electrical properties of a new structure-doubly eccentric cylindrical quantum wire. There is no report on electronic states of a doubly eccentric cylinder in nano regime to our knowledge. A doubly eccentric cylindrical quantum wire consists of two eccentric cylindrical quantum wire nested inside a cylindrical quantum wire of larger radius. A cross-section of such quantum wire is shown in Fig.1. Such doubly eccentric cylindrical wire in nano regime can help to develop semiconductor material to enhance the efficiency of many quantum devices. The electronic states in a doubly cylindrical hetrostructures with C_{2v} symmetry in soft wall confinement (SWC) are studied theoretically in this paper. As its limiting behavior, the corresponding electronic states in hard wall confinement (HWC) and massive wall confinement (MWC) are also obtained. An exact solution of effective mass Schrödinger equation is obtained by using addition theorem for shifting origin of cylindrical Bessel functions in hetrostructures to satisfy corresponding boundary conditions for wavefunctions. The validity of addition theorem in doubly eccentric cylinder imposes a restriction on the range of its eccentricity but that doesn't lead to an issue as allowed range of eccentricity to cover most of practical problems.

Section 2 of this paper presents general geometrical structure of the problem and its exact solution in soft wall confinement (SWC). At first, the solution of effective mass Schrödinger equation is obtained in terms of cylindrical Bessel functions for various regions. Effective mass boundary conditions are then applied across each pair of boundaries. Fourier expansion is applied on the expression obtained after applying appropriate boundary condition to get the solution in analytical form. As a result, these give a set of infinite simultaneous equations which is discussed in section 3. A determinant equation is obtained for non-trivial solution of the infinite simultaneous equations. The roots of this determinant equation give various energy eigenvalues. The lowest root of determinant equation is obtained numerically to get ground state energy. The separation between axes of two eccentric cylinders is termed as eccentricity of structure. The ground state energy is calculated by varying eccentricity of structure. The result in variation of ground state energy with eccentricity is presented graphically. The corresponding limiting solution for massive wall confinement (MWC) and hard wall confinement (HWC) is discussed in section 4. Section 5 presents concluding remarks.

2. Solution

Fig. 1 shows annular cross-section of a doubly eccentric cylindrical structure. The length is along Z -axis which is perpendicular to plane of figure. The axes of region I, II and III are parallel. Radii of regions I and III are 'a' and that of region II is 'b'. The separation between centres of region II and III is d_1 and that between I and II is d_2 . In the structure, it

is kept $d_1 = d_2 = d$ so that structure has C_{2v} symmetry which is more useful in physical applications. However, this methodology can be used to study the electronic states in doubly eccentric cylinder with $d_1 \neq d_2$ as well. The parameter ‘ d ’ represents separation between axes of inner cylinder and is called eccentricity.

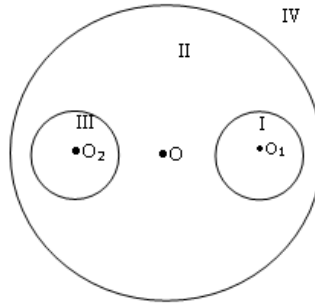


Fig. 1. Cross-section of a doubly eccentric cylinder.

We have considered a system in which an electron is free to move along axis of cylinder in region II and its annular motion is confined by different cylindrical barriers shown as regions I, III and IV in Fig. 1. Using the theory of effective mass approximation, each region can be considered as region of constant potential with corresponding effective mass of the electron. Let effective mass of the electron in l^{th} region is m_l^* , $l = 1, 2, 3$ and 4. We have set the value of potential energy of region II equal to zero as the reference of potential energy. Let the barrier potential in l^{th} region is $U_l (> 0)$, $l = 1, 3$ and 4. Taking (ρ_1, φ_1, z_1) as cylindrical polar co-ordinates with respect to origin O_1 , the effective mass Schrödinger equation [17-18] for hetrostructures is given as

$$\left[-\frac{\hbar^2}{2} \nabla \left\{ \frac{1}{m^*(\rho_1, \varphi_1, z_1)} \nabla \right\} + U(\rho_1, \varphi_1, z_1) \right] \psi(\rho_1, \varphi_1, z_1) = E\psi(\rho_1, \varphi_1, z_1) \tag{1}$$

For uniform distribution of effective mass m_l^* in the l^{th} region, $m_l^*(\rho_1, \varphi_1, z_1) = m_l^*$, the Eq. (1) takes the form

$$\nabla^2 \psi(\rho_1, \varphi_1, z_1) = -\frac{2m_l^*(E - U)}{\hbar^2} \psi(\rho_1, \varphi_1, z_1) \tag{2}$$

In region I, the solution of Eq. (2) with origin at O_1 comes as

$$\psi_I(\rho_1, \varphi_1, z_1) = \sum_{m=0}^{\infty} A_m I_m(k_1 \rho_1) \sin(m\varphi_1 + \phi_0) e^{i\beta z_1} \tag{3}$$

$$\text{with } k_1^2 = -\frac{2m_1^*(E - U_1)}{\hbar^2} + \beta^2 \tag{4}$$

where A_m are unknown constants, $I_m(k_1 \rho_1)$ is modified Bessel function of first kind, β is axial wave number and $\phi_0 = 0$ gives odd parity and $\phi_0 = \frac{\pi}{2}$ gives even parity.

In region II, the solution of Eq. (2) with origin at O_1 comes as

$$\psi_{II}(\rho_1, \varphi_1, z_1) = \sum_{m=0}^{\infty} (B_m J_m(k_2 \rho_1) + C_m Y_m(k_2 \rho_1)) \sin(m\phi_1 + \phi_0) e^{i\beta z_1} \quad (5)$$

$$\text{with } k_2^2 = \frac{2m_2^* E}{\hbar^2} - \beta^2 \quad (6)$$

where B_m and C_m are unknown constants, $J_m(k_2 \rho_1)$ is Bessel function of first kind and $Y_m(k_2 \rho_1)$ is Bessel function of second kind.

In region III, the solution of Eq. (2) with origin at O_1 comes as

$$\psi_{III}(\rho_1, \varphi_1, z_1) = \sum_{m=0}^{\infty} (D_m I_m(k_3 \rho_1) + E_m K_m(k_3 \rho_1)) \sin(m\phi_1 + \phi_0) e^{i\beta z_1} \quad (7)$$

$$\text{with } k_3^2 = -\frac{2m_3^* (E - U_3)}{\hbar^2} + \beta^2 \quad (8)$$

where D_m and K_m are unknown constants, $I_m(k_3 \rho_1)$ and $K_m(k_3 \rho_1)$ are modified Bessel function of first and second kind respectively.

In region IV, the solution of Eq. (2) with origin at O_1 comes as

$$\psi_{IV}(\rho_1, \varphi_1, z_1) = \sum_{m=0}^{\infty} F_m K_m(k_4 \rho_1) \sin(m\phi_1 + \phi_0) e^{i\beta z_1} \quad (9)$$

$$\text{with } k_4^2 = -\frac{2m_4^* (E - U_4)}{\hbar^2} + \beta^2 \quad (10)$$

Eq. (3) to Eq. (9) give the wavefunctions with some unknown constants in region I to IV respectively. These unknown constants and hence energy eigenvalues can be calculated using the fact that Ψ and $\frac{1}{m^*} \nabla \Psi$ (effective mass boundary condition) has to be continuous at each of the boundaries [19]. To apply boundary conditions across boundary between region I and II, wavefunctions ψ_I and ψ_{II} in terms of (ρ_1, φ_1, z_1) with origin at O_1 is good enough but for boundary between region II and III, wavefunctions ψ_{II} and ψ_{III} should be re-written in terms of new cylindrical polar co-ordinates (ρ_2, φ_2, z_2) with respect to origin at O_2 . Again for boundary between region II and IV, wavefunctions ψ_{II} and ψ_{IV} should be re-written in terms of (ρ, φ, z) with respect to origin at O . Addition theorem has been used to write the mathematical expression of wavefunction with origin shifted at ‘O’ or ‘ O_2 ’ from ‘ O_1 ’ as required during application of boundary conditions [20-23].

2.1. Boundary conditions between region I and II

The two boundary conditions required to be satisfied at $\rho_1 = a$ for all φ_1 and z_1 are

$$\psi_I = \psi_{II} \quad (11)$$

$$\text{and } \frac{1}{m_1^*} \nabla \psi_I = \frac{1}{m_2^*} \nabla \psi_{II} \tag{12}$$

Substituting Eq. (3) and Eq. (5) into Eq. (11) gives for each m

$$A_m = \frac{B_m J_m(k_2 a) + C_m Y_m(k_2 a)}{I_m(k_1 a)} \tag{13}$$

and substituting Eq. (3) and Eq.(5) into Eq. (12) gives for each m

$$B_m = C_m \frac{H_m(k_1, k_2)}{G_m(k_1, k_2)} \tag{14}$$

where

$$G_m(k_1, k_2) = \frac{1}{m_1^*} [k_1 m_2^* I_m'(k_1 a) J_m(k_2 a) - k_2 m_1^* I_m(k_1 a) J_m'(k_2 a)] \tag{15}$$

and

$$H_m(k_1, k_2) = \frac{1}{m_1^*} [k_2 m_1^* I_m(k_1 a) Y_m'(k_2 a) - k_1 m_2^* I_m'(k_1 a) Y_m(k_2 a)] \tag{16}$$

2.2. Boundary conditions between region II and III

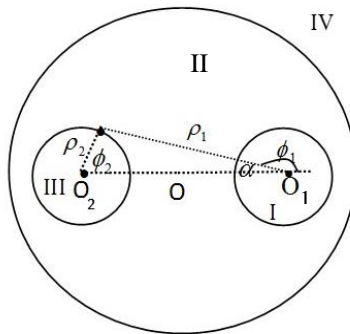


Fig. 2. For shift of origin from O₁ to O₂.

If (ρ_2, ϕ_2, z_2) is cylindrical polar co-ordinate with origin at O₂, the boundary conditions required to be satisfied at $\rho_2 = a$ for all ϕ_2 and z_2 are

$$\psi_{II} = \psi_{III} \tag{17}$$

$$\text{and } \frac{1}{m_2^*} \nabla \psi_{II} = \frac{1}{m_3^*} \nabla \psi_{III} \tag{18}$$

To apply boundary conditions given by Eq. (17) and Eq. (18), we need to shift origin from O₁ to O₂ using addition theorem. Within the range of d as $\frac{a}{2} \leq d \leq b - a$, the use of addition theorem with $\alpha = \pi - \phi_1$ (in Fig.2) gives

$$Z_m(k_2\rho_1)\sin(m\varphi_1+\varphi_0)=(-1)^{m+1}\cos(2\phi_0)\sum_{p=-\infty}^{p=\infty}Z_{m+p}(k_2d_{12})J_p(k_2\rho_2)\sin(p\varphi_2+\varphi_0), \quad (19)$$

where $Z = J$ or Y .

$$K_m(k_3\rho_1)\sin(m\varphi_1+\varphi_0)=(-1)^{m+1}\cos(2\phi_0)\sum_{p=-\infty}^{p=\infty}K_{m+p}(k_3d_{12})I_p(k_3\rho_2)\sin(p\varphi_2+\varphi_0) \quad (20)$$

$$\text{and } I_m(k_3\rho_1)\sin(m\varphi_1+\varphi_0)=(-1)^{m+1}\cos(2\phi_0)\sum_{p=-\infty}^{p=\infty}(-)^p I_{m+p}(k_3d_{12})I_p(k_3\rho_2)\sin(p\varphi_2+\varphi_0) \quad (21)$$

Using Eq. (5) and Eq. (19), the wavefunctions in region II about origin O_2 comes as

$$\begin{aligned} \psi_{II}(\rho_2, \varphi_2, z_2) = \\ \sum_{m=0}^{\infty} \sum_{p=-\infty}^{p=\infty} (-1)^{m+1} \cos(2\phi_0) [B_m J_{p+m}(k_2d_{12}) + C_m Y_{p+m}(k_2d_{12})] J_p(k_2\rho_2) \sin(p\varphi_2 + \phi_0) e^{i\beta z_2} \end{aligned} \quad (22)$$

and using Eq. (20), Eq. (21) and Eq. (7), the wavefunction in region III about origin O_2 comes as

$$\begin{aligned} \psi_{III}(\rho_2, \varphi_2, z_2) = \\ \sum_{m=0}^{\infty} \sum_{p=-\infty}^{p=\infty} (-1)^{m+1} \cos(2\phi_0) [(-)^p D_m I_p(k_3d_{12}) + E_m K_p(k_3d_{12})] I_{p-m}(k_3\rho_2) \sin(p\varphi_2 + \phi_0) e^{i\beta z_2} \end{aligned} \quad (23)$$

Substituting the ψ_{II} and ψ_{III} given by Eq. (22) and Eq. (23) into boundary conditions given by Eq. (17) and Eq. (18) and then expanding $\sin(p\varphi_2 + \phi_0)$ as Fourier series in ϕ_2 and then using Eq.(14) yields a set infinite simultaneous equations in C_m 's as

$$\sum_{n=0}^{\infty} \sum_{m=0}^{\infty} P_{nm} C_m = 0 \quad (24)$$

where

$$P_{mn} = [H_m(k_1, k_2) \alpha_{mn}(k_2, d_{12}) + G_m(k_1, k_2) \beta_{mn}(k_2, d_{12})] U_n(k_2, k_3) \quad (25)$$

$$\text{with } U_n(k_2, k_3) = [k_2 m_3^* J'_n(k_2 a) I_n(k_3 a) - k_3 m_2^* J_n(k_2 a) I'_n(k_3 a)] \quad (26)$$

$$\alpha_{mn}(k_2, d_{12}) = [J_{n+m}(k_2 d_{12}) + (-1)^{m-1} \cos(2\phi_0) J_{n-m}(k_2 d_{12})] \quad (27)$$

$$\text{and } \beta_{mn}(k_2, d_{12}) = [Y_{n+m}(k_2 d_{12}) + (-1)^{m-1} \cos(2\phi_0) Y_{n-m}(k_2 d_{12})] \quad (28)$$

2.3. Boundary conditions between region II and IV

If (ρ, φ, z) is cylindrical polar co-ordinate with origin at O, the boundary conditions required to be satisfied at $\rho = b$ for all ϕ and z are

$$\psi_{II} = \psi_{IV} \quad (29)$$

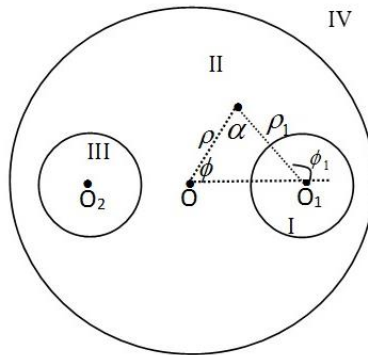


Fig. 3. For shift of origin from O_1 to O_2 .

$$\text{and } \frac{1}{m_2^*} \nabla \psi_{II} = \frac{1}{m_4^*} \nabla \psi_{IV} \tag{30}$$

To apply boundary conditions given by Eq. (29) and Eq. (30) between region II and IV, ψ_{II} and ψ_{IV} need to be written in cylindrical polar co-ordinates (ρ, φ, z) with respect to origin at O. Using addition theorem, the relation between Bessel functions in co-ordinates (ρ, φ, z) and (ρ_1, φ_1, z_1) with $\alpha = \phi_1 - \phi$ (in Fig.3) comes as

$$Z_m(k_2\rho_1)\sin(m\varphi_1 + \varphi_0) = \sum_{p=-\infty}^{p=\infty} Z_p(k_2\rho)J_{p-m}(k_2d)\sin(p\varphi + \varphi_0), \tag{31}$$

where $Z = J$ or Y

$$\text{and } K_m(k_4\rho_1)\sin(m\varphi_1 + \varphi_0) = \sum_{p=-\infty}^{p=\infty} K_p(k_4\rho)I_{p-m}(k_4d)\sin(p\varphi + \varphi_0) \tag{32}$$

Using Eq. (5) and Eq. (31), wavefunction in region II about origin O comes as

$$\psi_{II}(\rho, \varphi, z) = \sum_{m=0}^{\infty} \sum_{p=-\infty}^{p=\infty} [B_m J_p(k_2\rho) + C_m Y_p(k_2\rho)] J_{p-m}(k_2d) \sin(p\varphi + \phi_0) e^{i\beta z} \tag{33}$$

And, using Eq. (7) and Eq. (32), the wavefunction IV about origin O comes as

$$\psi_{IV}(\rho, \varphi, z) = \sum_{m=0}^{\infty} \sum_{p=-\infty}^{p=\infty} F_m K_p(k_4\rho) I_{p-m}(k_4d) \sin(p\varphi + \phi_0) e^{i\beta z} \tag{34}$$

Substituting the ψ_{II} and ψ_{IV} given by Eq. (33) and Eq. (34) into boundary conditions given by Eq. (29) and Eq. (30) and expanding $\sin(p\varphi + \phi_0)$ as Fourier series in ϕ and then using Eq. (14) yields a set infinite simultaneous equations in C_m 's as

$$\sum_{n=0}^{\infty} \sum_{m=0}^{\infty} Q_{mn} C_m = 0 \tag{35}$$

where

$$Q_{mn} = [H_m(k_1, k_2)S_n(k_2, k_4) + G_m(k_1, k_2)T_n(k_2, k_4)]W_{mn}(k_2d) \tag{36}$$

$$\text{with } S_n(k_2, k_4) = [k_2m_4^* J_n'(k_2b)K_n(k_4b) - k_4m_2^* J_n(k_2b)K_n'(k_4b)] \tag{37}$$

$$T_n(k_2, k_4) = [k_2m_4^* K_n(k_4b)Y_n'(k_2b) - k_4m_2^* K_n'(k_4b)Y_n(k_2b)] \tag{38}$$

$$\text{and } W_{mn}(k_2d) = J_{n-m}(k_2d) + (-1)^{m+1} \cos 2\varphi_0 J_{n+m}(k_2d) \tag{39}$$

3. Results and Discussion

The Eq. (24) and Eq. (35) are infinite simultaneous equation in C_m 's and can be expanded as

$$\begin{aligned} P_{11}C_1 + P_{21}C_2 + P_{31}C_3 + \dots &= 0 \\ P_{12}C_1 + P_{22}C_2 + P_{32}C_3 + \dots &= 0 \\ P_{13}C_1 + P_{23}C_2 + P_{33}C_3 + \dots &= 0 \\ \dots & \\ \dots & \\ Q_{11}C_1 + Q_{21}C_2 + Q_{31}C_3 + \dots &= 0 \\ Q_{12}C_1 + Q_{22}C_2 + Q_{32}C_3 + \dots &= 0 \\ Q_{13}C_1 + Q_{23}C_2 + Q_{33}C_3 + \dots &= 0 \\ \dots & \end{aligned}$$

For non-trivial solution of C_m 's, the determinant of co-efficient in above equations should be equal to zero. Therefore,

$$\det \begin{vmatrix} \tilde{P} \\ \tilde{Q} \end{vmatrix} = 0 \tag{40}$$

Where, \tilde{P} and \tilde{Q} are transpose of corresponding matrices given by the Eq. (25) and Eq. (36) respectively. For a given SWC, the solution of Eq. (38) will be a polynomial equation in energy eigenvalues E which various roots will give energy eigenvalues of the system. By increasing the order of determinates, the roots converges to specific values. The lowest root gives ground state energy. The lowest root is obtained numerically which converges to third decimal places for 10×10 determinant entries in Eq. (40). Considering region II is made of GaAs and all other regions I, III and IV are made of $\text{Ga}_{0.7}\text{Al}_{0.3}\text{As}$, we have taken $m_1^* = m_3^* = m_4^* = 1.4m_2^*$, $m_2^* = 5.73 \times 10^{-32} \text{ kg}$. For fixed radii $a = 6 \text{ nm}$ and $b = 20 \text{ nm}$, barrier potential energies $U_1 = U_3 = U_4 = 190 \text{ meV}$ and setting $\beta = 0$, the ground state energy is calculated by solving numerically Eq. (40) with 10×10 entries for varying eccentricity $d = 4 \text{ nm}$ to 13 nm (within allowed range for d according to used addition theorem in methodology). The result is shown graphically in Fig. 4. The decrease in ground state energy with increase in eccentricity can be justified as result of Uncertainty principle.

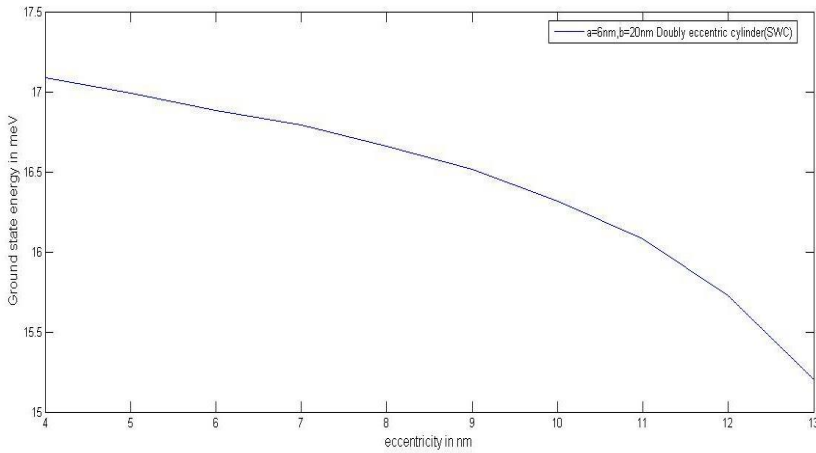


Fig. 4. Variation of ground state energy with eccentricity.

4. Limiting Behavior

4.1. Massive wall confinement (MWC)

The energy eigenvalues of the system under MWC can be obtained by applying the limit $\frac{m_i^*}{m_2^*} \rightarrow \infty, i = 1, 3$ and 4 during obtaining the solution in section II for SWC. Boundary conditions will now ensure that the quantity $\frac{1}{m_2^*} \nabla \psi_{II} = 0$ at each boundary between different regions [24]. Repeating the same procedure as in Section II with limit $\frac{m_i^*}{m_2^*} \rightarrow \infty, i = 1, 3$ and 4, yields two sets of infinite simultaneous equations in C_m 's as

$$\sum_{n=0}^{\infty} \sum_{m=0}^{\infty} P_{mn}^{MWC} C_m = 0 \tag{41}$$

$$\sum_{n=0}^{\infty} \sum_{m=0}^{\infty} Q_{mn}^{MWC} C_m = 0 \tag{42}$$

where

$$P_{mn}^{MWC} = \begin{bmatrix} J'_m(k_2 a) \{ Y_{n+m}(k_2 d_{12}) + (-1)^{m-1} \cos(2\phi_0) Y_{n-m}(k_2 d_{12}) \} \\ -Y'_m(k_2 a) \{ J_{n+m}(k_2 d_{12}) + (-1)^{m-1} \cos(2\phi_0) J_{n-m}(k_2 d_{12}) \} \end{bmatrix} J'_n(k_2 a) \tag{43}$$

$$\text{and } Q_{mn}^{MWC} = [J'_m(k_2 a) Y'_n(k_2 b) - J'_n(k_2 b) Y'_m(k_2 a)] W_{mn}(k_2 d) \tag{44}$$

$$\text{with } W_{mn}(k_2d) = J_{n-m}(k_2d) + (-1)^{m+1} \cos 2\phi_0 J_{n+m}(k_2d) \tag{45}$$

For non-trivial solution of Eq. (41) and Eq. (42),

$$\det \begin{vmatrix} \tilde{P}^{MWC} \\ \tilde{Q}^{MWC} \end{vmatrix} = 0 \tag{46}$$

Where, \tilde{P}^{MWC} and \tilde{Q}^{MWC} is transpose of the corresponding matrices given by Eq. (43) and Eq. (44) respectively.

4.2. Hard wall confinement (HWC)

Under the limit that barrier potential energies (potential energies of region I, III and IV) are infinite, wavefunction ψ_{II} should vanish at each of the boundary between different regions. Repeating the same procedure discussed in the section II under the boundary condition $\psi_{II} = 0$ at each of the boundaries yields two sets of infinite simultaneous equations in C_m 's as

$$\sum_{n=0}^{\infty} \sum_{m=0}^{\infty} P^{HWC}_{mn} C_m = 0 \tag{47}$$

$$\sum_{n=0}^{\infty} \sum_{m=0}^{\infty} Q^{HWC}_{mn} C_m = 0 \tag{48}$$

where

$$P^{HWC}_{mn} = \begin{bmatrix} J_m(k_2a) \{ Y_{n+m}(k_2d_{12}) + (-1)^{m-1} \cos(2\phi_0) Y_{n-m}(k_2d_{12}) \} \\ -Y_m(k_2a) \{ J_{n+m}(k_2d_{12}) + (-1)^{m-1} \cos(2\phi_0) J_{n-m}(k_2d_{12}) \} \end{bmatrix} J_n(k_2a) \tag{49}$$

$$\text{and } Q^{HWC}_{mn} = [J_m(k_2a) Y_n(k_2b) - J_n(k_2b) Y_m(k_2a)] W_{mn}(k_2d) \tag{50}$$

$$\text{with } W_{mn}(x) = J_{n-m}(x) + (-1)^{m+1} \cos 2\phi_0 J_{n+m}(x) \tag{51}$$

For non-trivial solution of Eq. (47) and Eq. (48),

$$\det \begin{vmatrix} \tilde{P}^{HWC} \\ \tilde{Q}^{HWC} \end{vmatrix} = 0 \tag{52}$$

Where, \tilde{P}^{HWC} and \tilde{Q}^{HWC} is transpose of the corresponding matrices given by Eq. (49) and Eq. (50) respectively.

5. Conclusion

A general technique to study electronic states in doubly eccentric cylindrical quantum wire for soft wall confinement has been presented. Massive wall confinement and hard

wall confinement is presented as its limiting case. The ground state energy of the structure is calculated. The variation in ground state energy with eccentricity is obtained numerically. The ground state energy is found to be decreases with increase in eccentricity of structure. One can similarly find numerically other higher roots of determinant equation to study excited states as well. The discussed method can be also further used to study having more than two similar or different cylindrical barriers nested in it in nano regime.

References

1. M. Toshipa, Adv. Cond. Matter Phys. **2019**, ID 3478506 (2019). <https://doi.org/10.1155/2019/3478506>
2. P. Kumari, S. Sinha, and L. K. Mishra, J. Pure Appl. Indus. Phys. **7**, 264 (2017).
3. A. J. Peter and J. Ebenezar, J. Sci. Res. **1**, 200 (2009). <https://doi.org/10.3329/jsr.v1i2.1184>
4. B. Choupanzadeh, H. Kaatuzian, R. Kohandani, and S. Abdolhosseini, Optics Photonics J. **6**, 114 (2016). <https://doi.org/10.4236/opj.2016.68B019>
5. C. Tablero, J. Appl. Phys. **106**, ID 074306 (2009). <https://doi.org/10.1063/1.3243290>
6. V. I. Boichuk, I. V. Bilynskiy, O. A. Sokolnyk, and I. O. Shakleina, Cond. Matter Phys. **16**, ID 33702 (2013). <https://doi.org/10.5488/CMP.16.33702>
7. C. Tablero, J. Chem. Phys. **122**, ID 064701 (2005). <https://doi.org/10.1063/1.1844395>
8. C. Y. Ngo, S. F. Yoon, W. J. Fan, and S. J. Chua, Phys. Rev. B **74**, ID 245331 (2006). <https://doi.org/10.1103/PhysRevB.74.245331>
9. M. Masale, Physica E: Low-dimensional Systems Nanostruct. **5**, 98 (1999). [https://doi.org/10.1016/S1386-9477\(99\)00029-6](https://doi.org/10.1016/S1386-9477(99)00029-6)
10. M. Masale, Physica Scripta **65**, 459 (2002). <https://doi.org/10.1238/Physica.Regular.065a00459>
11. S. Yu and K. W. Kim, J. Appl. Phys. **80**, 2815 (1996). <https://doi.org/10.1063/1.363199>
12. M. Roy and P. A. Maksym, Phys. Rev. B **68**, ID 235308 (2003). <https://doi.org/10.1103/PhysRevB.68.235308>
13. S. D. Sarma and E. H. Hwang, Phys. Rev. B **54**, ID 1936 (1996). <https://doi.org/10.1103/PhysRevB.54.1936>
14. K. A. Matveev, Phys. Rev. B **70**, ID 245319 (2004). <https://doi.org/10.1103/PhysRevB.70.245319>
15. C. Pryor, Phys. Rev. B **44**, 12912 (1991). <https://doi.org/10.1103/PhysRevB.44.12912>
16. S. K. Dey, S. N. Singh, A. Kapoor, and G. S. Singh, Phys. Rev. B **67**, ID 113304 (2003). <https://doi.org/10.1103/PhysRevB.67.113304>
17. G. T. Einevoll, P. C. Hemmer, and J. Thomson, Phys. Rev. B **42**, ID 3485 (1990). <https://doi.org/10.1103/PhysRevB.42.3485>
18. G. T. Einevoll, Phys. Rev. B **42**, ID 3497 (1990). <https://doi.org/10.1103/PhysRevB.42.3497>
19. G. Bastard, Wave Mechanics Applied to Hetrostructures Semiconductor (Les Ulis: Lees Editions de Physique, 1988) pp. 112.
20. G. N. Watson, A Treatise on the Theory of the Bessel Functions (Cambridge University, London, 1958) pp. 361.
21. G. S. Singh and S. N. Singh, J. Math. Phys. **30**, 829 (1989). <https://doi.org/10.1063/1.528405>
22. G. S. Singh and L. S. Kothari, J. Math. Phys. **25**, 810 (1984). <https://doi.org/10.1063/1.528405>
23. S. N. Singh and G. S. Singh, J. Math. Phys. **35**, 3230 (1994). <https://doi.org/10.1063/1.530463>
24. P. C. Hemmer and D. T. Wang, Phys. Rev. B **47**, ID 6603 (1993). <https://doi.org/10.1103/PhysRevB.47.6603>